

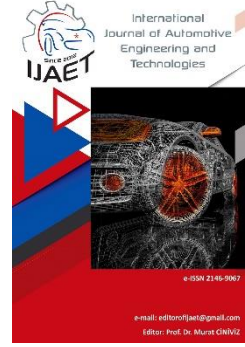


e-ISSN: 2146 - 9067

International Journal of Automotive Engineering and Technologies

journal homepage:

<https://dergipark.org.tr/en/pub/ijaet>



Original Research Article

Design and optimization of runner and gating systems, in high-pressure casting and sand casting, for an aluminum alloy valve cover



Alen Murat Kuyumcu^{1,*}, Yuşa Haktanır²

^{1*,2} Beykent University, Faculty of Engineering and Architecture, Mechanical Engineering, İstanbul, Türkiye.

ARTICLE INFO

Orcid Numbers

1. 0000-0002-6396-5315

2. 0000-0002-4808-7390

Doi: 10.18245/ijaet.1200972

* Corresponding author

alenkuyumcu@yahoo.com

Received: Nov 08, 2022

Accepted: Nov 14, 2023

Published: 31 Dec 2023

Published by Editorial Board Members of IJAET

© This article is distributed by Turk Journal Park System under the CC 4.0 terms and conditions.

ABSTRACT

The weight and speed advantage of aluminum die-casting leads to its use in many parts in the automotive industry. Casting simulation programs are used, to avoid time-consuming and expensive production costs, and to design the production process. For casting production one of the most important factors is the runner design, which directly affects castability, material selection, and casting quality. With the correct design of runner systems, there will be no problem with the casting part. In this study, the final part and the runner design for the aluminum alloy valve cover were modeled in CAD, according to the empirical calculations. Furthermore, an appropriate casting method was selected for the valve cover not only according to the results of both high-pressure die-casting and sand-casting simulations but also economic calculations. The main technical parameters for selection were mold and part temperature distribution, liquid metal flow rates, cold shut possibilities, final air quantities, microporosity, and microporosity values. After the final decision, the casting part was produced with high pressure die casting by the implementation of the final runner design.

Keywords: High pressure die casting, Sand casting, Casting simulation, Runner design, Aluminum alloy

1. Introduction

The high-pressure die casting (HPDC) method is used in many sectors today, especially in processes that have complex structures and require many similar parts to be produced. Thus, the production of complex parts from the outside and inside can be performed without any machining process. Manufactured parts are obtained for mass production because of their high repeatability. Parts and components of a large and complex structure can be

economically produced using the high-pressure casting method, whereas their production is not possible using another manufacturing process. The injection molding method is a production method that allows the production of complex parts by melting and molding the material at high temperatures. The most important difference that distinguishes injection molding from other production methods is that the parts produced by injection molding do not require finishing operations; even if there is, this is a very rare condition.

Nowadays, small and large parts are produced by the injection molding method. HPDC accounts for almost 70% of aluminum components manufactured today [13]. Many aluminum components for the automotive industry are cast using this method because of its high productivity and near net shape production. Large components, such as gearbox housings and engine blocks, are typical examples of casting weights exceeding 15 kg. Because of the short cycle times, the die is exposed to high temperature fluctuations during each casting cycle, resulting in steep thermal gradients on and below the surface of the die [14]. With HPDC, molten metal is forced into the die cavity under pressure. Because of the high speed of metal filling and rapid solidification rate, this casting process is commonly used to manufacture high-volume, thin-walled castings rather than using other die casting methods, such as gravity or low pressure. Non-ferrous alloys, mainly aluminum, magnesium, and zinc, are most commonly cast using this process. [12]

Many casting methods are used, which are selected depending on the weight of the part, required surface quality, production quantities, and costs. Currently, sand casting (SC) is usually used in the production of casting parts at the prototype stage, whereas other casting methods are used in the production of mass-production parts by casting.

Zheng et al. stated that a good casting simulation should be used to improve casting quality and that simulation programs should reduce cost. They simulated the casting process of a copper alloy water flow meter produced by sand casting while focusing on the effects of different runner designs for optimized casting [10]. Kumar et al. used ProCast to design gating systems for rotary adaptor defect minimization [11]. Hu et al. performed numerical simulations of the design and optimization of runner and gating systems for die-casting thin-walled magnesium telecommunication parts. Two types of runner and gating systems were designed. Suresha and Pawan used Z-cast to design the mold and gate system for a heat sink [1]. Ramnath et al. performed analytic calculations in high-pressure casting for the design of the runner

and confirmed the results by casting simulation [5]. Sulaiman and Keen performed flow analysis along the runner and gating system of a casting process using four gates and the angles of the branches leading to the gate [6]. Yang et. al. pointed out the importance of runner design to the mechanical strength of Al-7Si-Mg alloy castings by not only CFD analysis and X-ray radiography [8]. In addition, the four-point bending method was applied. Both numerical and experimental results showed that the vortex-flow runner system (VR) could effectively control the ingate velocity and keep its value lower than 0.5 m/s. As seen above, casting simulations are used more commonly day by day to ensure the quality and optimum production of parts in foundries. It is a great advantage to use casting simulations to provide complex geometry, large volume, and high production quality. Using casting simulations, the percentage of parts scrapped can be decreased. In addition, labor costs and casting times can be optimized for the foundry. To obtain realistic values from the casting simulation, all customized parameters should be entered into the simulation program according to previous experience. If all conditions of the process are defined correctly as simulation inputs, it is possible to obtain values that correlate with real-life values. Casting simulations were used to improve the parts in the design phase and the outputs of the casting properties. If the selected casting method is not suitable for the part design, the design should be revised according to the casting method.

The basic design can be finalized by the inputs of FEA or MBS analysis, while the part design is finished, casting simulations should be applied. If needed, a loop can be examined between the FAE and casting simulations.

2. Methodology

In this study, the appropriate casting method for an aluminum alloy valve cover was selected on the basis of casting simulations. In addition, the runner design was investigated. The engine valve cover, which is the outcome of the project, and the runner were designed using the Catia V5R21 CAD program. The production process of the designed runners and casting parts was simulated using a casting simulation program

called Altair Inspire Cast. Runner designs were made according to the runner calculations and verified by casting simulation. The valve cover was designed with different wall thicknesses for high-pressure die-casting and sand-casting. According to the simulation results, the most suitable casting method was selected, considering casting weight, production time, casting quality, total cost, and scrap rate. The casting simulations were completed by optimizing the mold temperature, runner optimization, riser position, and material temperature distribution. According to Dubey and Smruti (2019), mold design starts with the definition of geometry and material, which are selected according to mechanical and chemical needs [11]. After this process, necessary design corrections can be made according to the molding angle and shrink factor, which is a material feature, and several mold cavities will be decided according to the number of parts that fit into the mold. In the next step, the runner geometry and the location of the inlet channel, which will allow the liquid metal to enter the mold, must be determined while the mold cavities are placed for optimum filling of the casting part. Figure 1 shows the Design methodology systematic of the casting part. This figure is created in the light of the methodology of Dubey and Smruti.

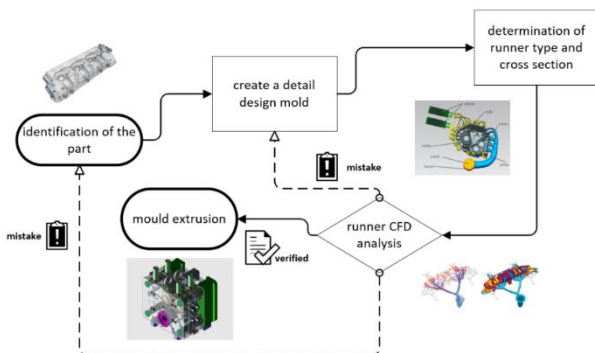


Fig. 1. Design methodology systematics of a casting part

3. Design parameters and calculations

The gating system and its design are the main parameters in the casting processes because they allow the liquid metal to enter the mold and determine the most important properties of the final product. An optimized runner design leads to less scrap and a more homogeneous material distribution. When liquid metal is poured into the mold, turbulence and splashes can occur. During each impact and splash, the molten metal

absorbs air, which causes casting voids or porosity on the casting part. Vertical and horizontal runners are generally used in the runner designs that we traditionally use. Different conical spouts in vertical runners and straightforward molten metal descending designs are also known. Conical filling nozzles are usually made of a wide and flat filling nozzle that allows the liquid metal to be easily filled into the mold.

3.1. Characteristics of the valve cover to be used in casting simulations

A valve cover protects engine parts such as rockers, valves, and springs from dust and outer effects and is also used for noise insulation and condensation of evaporated engine oil. They are usually produced from cast or sheet metal or thermoplastic. In this study, we developed two different valve cover designs to fulfill casting production limits. A design is suitable for the high-pressure die-casting method and the other is suitable for the sand-casting method. Not only will the features of these two designs be discussed separately, but there will also be differences in the runner designs. The decision on the appropriate casting process to produce the valve cover will be made according to the final price and product quality. The features of the valve cover used in the high-pressure die casting simulation are listed in Table 1, and those of the valve cover used in the sand-casting simulation are listed in Table 2.

Table 1. Features of the valve cover used in high-pressure die-casting simulation

Determination	Descriptions
Engine type	4 cylinders
Casting part weight	2.3 kg
LengthxWidthxHeight (mm)	~190 x ~513 x ~121
Material	EN AC-46000 (G-Al Si9Cu3)
Runner feed	Bottom feed

Table 3 provides the terminology and key numerical values employed in the calculations for designing runners in high-pressure die-casting. Similarly, Table 4 outlines the terminology and critical numerical parameters used in the design calculations for runners in sand casting.

3.2. High-pressure die-casting design calculations

Machine capacity can be determined as below;

Projected projection area (Ps) including overflow and supply system = AC x AF
 Total tonnage for locking =PS x Pi x safety coefficient from Ramnath et al (2014)
 According to this information;
 Total tonnage = 122,500 mm² x 320 bar x 10 x 1.05 ≈ 412T
 The tonnage required for locking is about 1.2 times the total tonnage.

Table 3. High-pressure diecasting nomenclature and critical numbers

Determination	Descriptions
d (plunger diameter)	75/80/85/90 mm
k (filling rate coefficient)	0.0346
Ti (Temperature of molten metal as it enters the die)	675°C
Tf (Minimum flow temperature of metal)	570°C
Td (Temperature of die cavity surface just before the metal enters)	160°C
S (percent solid fraction allowable in the metal at the end of filling)	25%
Z (The units conversion factor)	3.8
Casting average wall thickness	3 mm
Density	2.65x10 ⁻³ g/mm ³
The projected area of component (Ac)	1225 cm ²
Draft angle	2°
Angular Tolerance	±0.5°
Specific injection pressure (Pi)	320 bar
Factor of safety	1.05
Stroke length for 550T machine	480 mm
Fill ratio	0.50
1.phase velocity	25 cm/s
2.phase velocity	375 cm/s
Mold material	1.2343

Total tonnage required for locking = 412T * 1.2 ≈ 495T
 550t metal injection machine with a cold chamber can be selected according to the result.
 Stroke volume can be calculated as below; 126
 $V_c + V_{of} = 890,000 \text{ mm}^3 * 1.4 = 1,246,000 \text{ mm}^3$
 Vof: The volume of overflow and feed system, excluding biscuit volume
 Actual stroke volume (Vs) = 1,246,000 mm³ + $\pi * d^2 * h / 4 \text{ mm}^3$
 The stroke length for the 550-ton cold chamber injection machine is 480 mm; with a biscuit that has 15 mm thickness effective stroke will be decreased to 465 mm.
 Assuming a filling rate of 0.50.
 Volume offered by injection molding machine;

$$= \pi * d^2 * (465/4) * 0.5$$

$$1,246,000 + \pi * d^2 * (465/4) * 0.5 = \pi * d^2 * (465/4)$$

$$58 * \pi * d^2 = 1,246,000$$

$$d^2 \approx 6841.65$$

$$d \approx 82 \text{ mm}$$

The piston diameter was selected as 80 mm.
 According to Ramnath et al., the filling rate is defined as the ratio of metal volume to stroke distance [5]. In this work, filling rate was calculated as 0.53 which is an acceptable value.

Again, from same work filling time (FT) is calculated as;
 $FT = k * [Ti - Tf + s * z] * Tk / [Tf - Td]$
 $t = ((0.0346 * [675 - 570 + 25 * 3.8] * 3)) / (570 - 160)$
 $t = 0.05 \text{ sec.}$

Filling velocity (FV) can be defined as the ratio of liquid metal volume at nozzle inlet to filling time.

$FV = 1,246,000 / 0.05 \approx 24,920,000 \text{ mm}^3/\text{sec}$
 Total gate area (TGA) can be defined as the ratio of filling velocity to liquid metal velocity at gate inlet.

$$TGA = 24,920,000 \text{ mm}^3/\text{s} / 50,000 \text{ mm/s}$$

$$\text{Total nozzle area} \approx 498 \text{ mm}^2 / 5 \approx 100 \text{ mm}^2$$

Table 4. Sand casting nomenclature and critical numerical parameters

Determination	Descriptions
Ti (Temperature of molten metal as it enters the die)	750°C
Tf (Minimum flow temperature of metal)	562°C
Td (Temperature of die cavity surface just before the metal enters)	40°C
Casting average wall thickness	5 mm
Density	2.67x10 ⁻³ g/mm ³
Draft angle	3°
Angular Tolerance	±0.5°
Total casting weight	6.8 kg
Casting time	5 sec.
Mold material	Greensand casting
Coefficient of friction	0.4
Shrinkage (%)	3.4
The surface area of the casting section	4398.9 cm ²

Gate section diameter varies according to various materials. Table 5 shows the areas of the input cross-section thickness, which vary according to the materials in Ramnath et al (2014).

In the optimized runner design, the width of the gate cross-section was 1.25 mm, resulting in a total thickness of 395 mm. As we used 5 gates, each width should be 79 mm. On the other hand, the runner cross-sectional area can be defined as the double of the nozzle area, i.e., 200 mm² for the branches.

Table 5. areas of the input cross-section, which vary according to the materials from

Material	Gate Section thickness (mm)
Al-Si – alloy	1 – 1.4
Al-Si Cu – alloy	1.2-2.5
Zn Al4 – alloy	0.35-0.8
Zn Al4 Cu alloy	0.5-1.2
Mg Al2	0.6-2
58-60 brass	1.5-3

3.3. Sand casting design calculations

The height of the flask is selected as 190 mm and the height of the part is 125 mm.

Effective casting height

$$H_E = h - (c/2)$$

$$H_E = 19 \text{ cm} - (12.50 \text{ cm} / 2)$$

$$H_E = 12.75 \text{ cm}$$

Critical section (C_a);

$$\frac{22.6 \times W}{\rho \times \varepsilon \times t \times \sqrt{H_E}} = \frac{22.6 \times 6.8}{2.67 \times 0.4 \times 5 \times \sqrt{12.75}}$$

W: Total casting weight (kg)

$$\rho = \text{density (gr/cm}^3\text{)}$$

ε = coefficient of friction

t = casting time (sec)

H_E = effective casting height (cm)

$$C_a \approx 8 \text{ cm}^2 = 800 \text{ mm}^2$$

$$C_a, \text{ colon} = r^2 * \pi$$

$$800 \text{ mm}^2 = r^2 * 3.14$$

$$r \approx 16 \text{ mm then } \varnothing = 32 \text{ mm}$$

Horizontal runner section;

Because the cross-section of the horizontal runner is in a trapezoid profile;

$$800 \text{ mm}^2 = (a+2a)*2a / 2 = 3a^2$$

$$a \approx 16 \text{ mm}$$

Gate section; C_a x (1.1) \approx 800 x 1.1 \approx 880 mm²

Number of feeder gate 10 PCs.

$$880 \text{ mm}^2 / 10 = 88 \text{ mm}^2$$

In general, gate cross-section measurements are experienced in the form of u-4u or u-6u. From the simulation, the gate entry section is taken as

u-6u. If the feeder is to be used on the part, the feeder neck does not need to be calculated. According to Brown (1999), if the side feeder is used, it is obtained using MC:MN: MF = 1.0:1.1:1.2 ratio. Because the feeder will be used from the top of the valve cover to be simulated, the feeder neck is not calculated. To calculate the riser module, the component module must be calculated first.

$$M_c = VC / AC$$

$$M_c = 1000 \text{ cm}^3 / 4398.9 \text{ cm}^2 \approx 0.22$$

$$MF = 1.2 \times M_c$$

In the feeder module calculation formula, the safety factor is selected as 1.2 and the safety coefficient is selected as 1.8 which helps to increase the capacity of the feeder to eliminate shrinkage. MF = 1.8 x 0.22 \approx 0.4 was found and when the module value was entered in the simulation program, the feeder module diameter was designed as 24 mm. Feeder weight;

$$W_F = W_T \times 100 / C_c * S_s / 100$$

According to Brown (1999), the optimal feeder metal ratio for C_c is 33% when using a Foseco sleeve, 16% if using a live natural feeder, i.e., a feeder before reaching the liquid metal casting cavity, and 10-14% for another natural feeder.

$$W_F = 3.475 \text{ kg} * 100 / 14 * 3.4 / 100 \approx 0.8 \text{ kg}$$

3.4. Parts of high-pressure die casting and sand-casting process and runner design

In the runner design of the high-pressure die casting process, the casting part is fed with five gates, and chill vent-type ventilation and overflow pockets are used. The runner is designed with rounded lines to avoid sharp corners. The width of the runner was 20 mm, the narrowest area was 10 mm, and the thickness of the pouring basin was 1.25 mm. In the runner design of the sand-casting process, a part is fed with 6 gates without a riser. The offset pouring basin was evaluated according to the simulation results. Rounded lines are used to ensure that the liquid metal is not faced with any resistance when it is entangled in the mold. The width of the runner was 31 mm, the narrowest area was 16 mm, and the filling gate was 4 mm.

Figure 2 shows parts of the high-pressure die-casting process, and Figure 3 shows parts of the sand-casting process. Figure 4 shows a technical drawing of the runner design for high-pressure die casting, and Figure 5 shows a technical drawing of the runner design for sand casting.

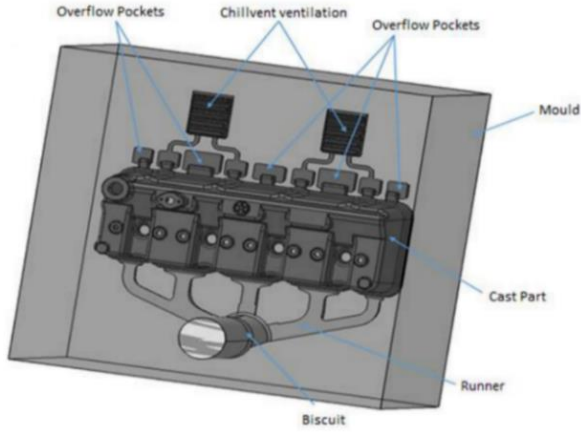


Fig. 2. Parts of the high pressure die casting process

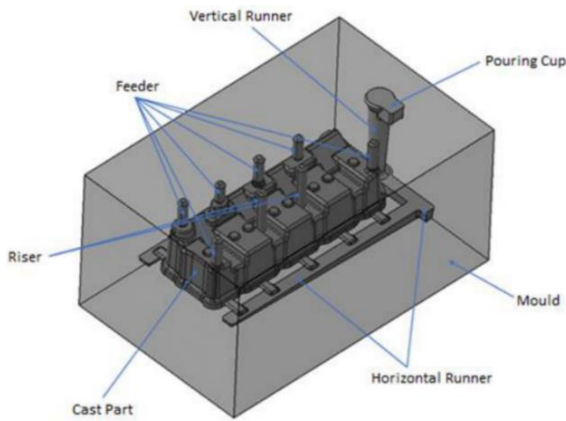


Fig. 3. Parts of the sand-casting process

4. Results and Discussion

These two casting methods have their advantages and disadvantages; however, in this section, a comparison will be performed according to the simulations of the aluminum alloy valve cover. When a well-calibrated casting simulation is used in accordance with the production process, errors in the preliminary design will emerge, and it will be possible to prevent losses such as mold material and labor costs.

4.1. Comparison of mold and part temperature distributions

In aluminum alloys, rapid cooling increases the strength of the casting part. In the literature. The main reason for this strength effect is the dendrite structure formed by the aluminum alloys during cooling. However, it is not correct to link increases in strength to the dendrite structure caused only by rapid cooling; it changes many parameters along with rapid cooling. Aluminum alloys begin to transform into the eutectic composition at approximately 555°C and exhibit high strength in this temperature range. In

aluminum casting alloys, solidification should occur at the temperature ranges instead of the constant temperature range. Low mold temperature reduces thermal stress and mold wear.

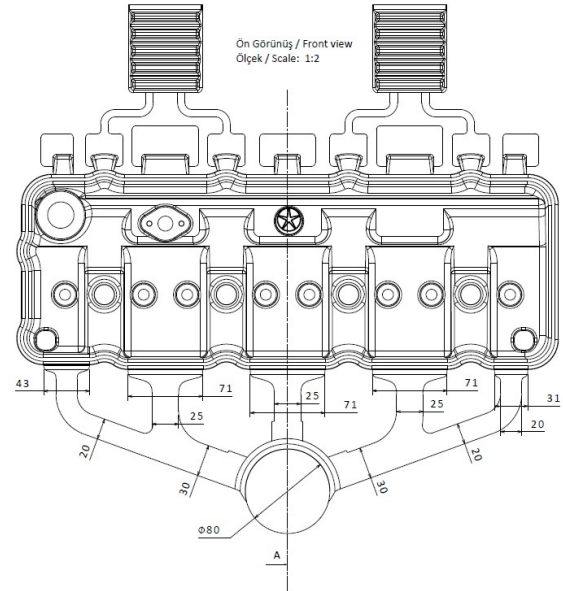


Fig. 4. Technical drawing of the runner to be produced by high-pressure die casting

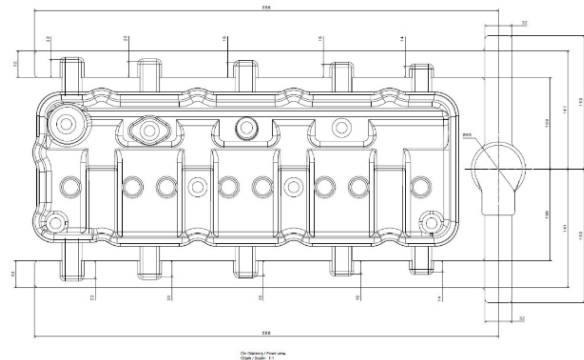


Fig. 5. Technical drawing of the runner to be produced by sand casting



Fig. 6. End of casting temperatures for high pressure die casting

In high-pressure die casting simulation, the maximum mold temperature is 439°C; however, in sand casting 500°C to 545°C. Figure 6 shows the end of casting temperature distribution for high-pressure die casting, and Figure 7 shows the end of casting temperatures for sand casting. Figure 8 shows the temperature distribution 30 s after the start of solidification of high-pressure casting, and Figure 9 shows the same parameter for sand casting. Figure 10 shows a graph of the temperature at the end of the casting for high-pressure casting. Figure 11 shows the same results for sand casting.

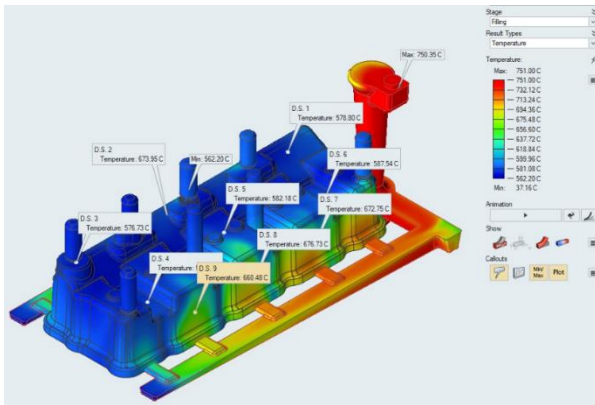


Fig. 7. End of casting temperatures for sand casting

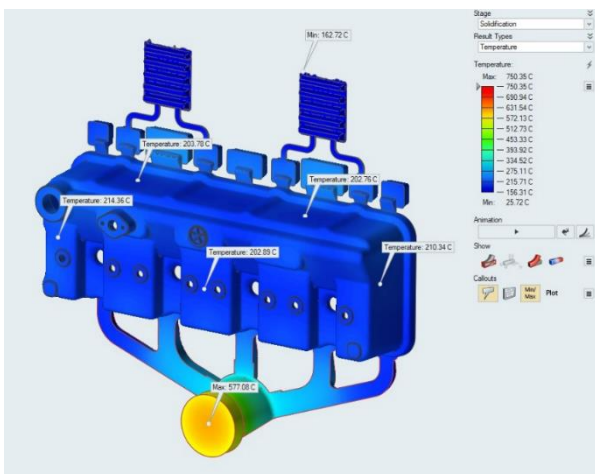


Fig. 8. Temperature 30 s after the start of solidification of high-pressure die casting



Fig. 9. Temperature 30 s after the start of solidification of the sand-casting part

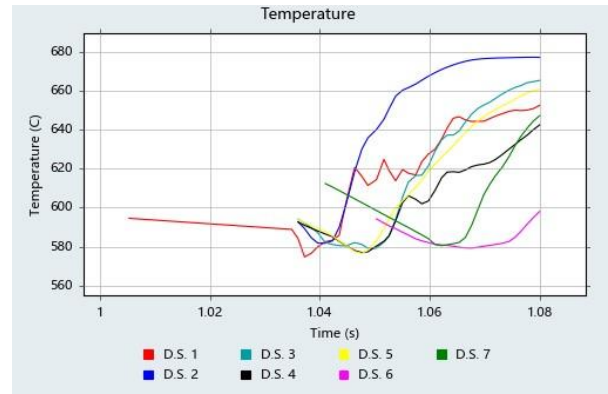


Fig. 10. Graph of the temperature for high-pressure die-casting part



Fig. 11. Graph of the temperature for sand casting part

Figure 12 shows a comparison of the minimum cast temperatures in the 30th second of solidification. Compared with the part temperature distributions, solidification occurs much faster in sand casting than in high-pressure die casting.

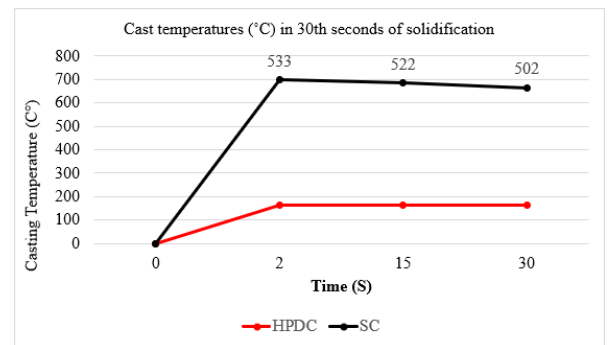


Fig. 12. Comparison of minimum cast temperatures (°C) in 30th seconds of solidification

4.2. Liquid metal flow rates comparison

When the literature is examined, for high-pressure die casting, liquid metal velocities in the gate part are between 30 and 60 m/s [2], whereas for sand casting, this limit is 0.5 m/s, as reported by Campbell (2003). In addition, surface tension for aluminum was taken as 0.914 N/m [8]. The critical velocity is calculated for sand casting. Consequently, the liquid metal velocities of both casting methods are acceptable. Figure 13 shows

the liquid metal velocities in the gate section of the high-pressure casting. Figure 14 shows the same results for sand casting.

$$V_{critical} = 2 * \sqrt[4]{\gamma g / \rho};$$

$$2 * \sqrt[4]{0.914 \frac{N}{m} * 9.81 m/s^2 / 2670 kg/m^3}$$

$$= 0.48 m/s$$

$$V_{critical}$$

$$= 2 * \sqrt[4]{\gamma g / \rho} * 2 * \sqrt[4]{0.914 \frac{N}{m} * 9.81 m/s^2 / 2670 kg/m^3}$$

Liquid metal velocity is not only within acceptable ranges in the sand-casting method but also within acceptable limits for high pressure die casting.

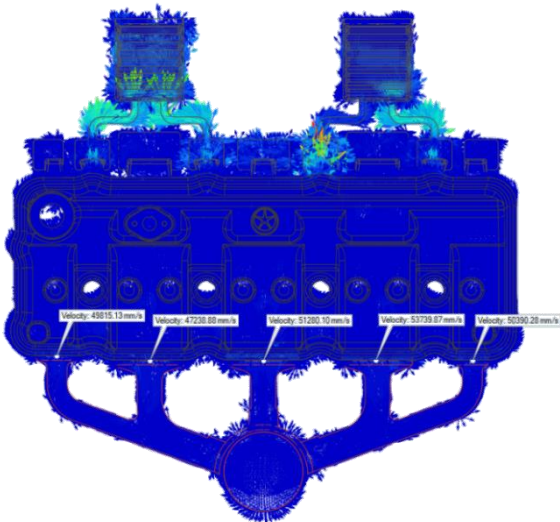


Fig. 13. Liquid metal velocities in the gate section of high-pressure die casting

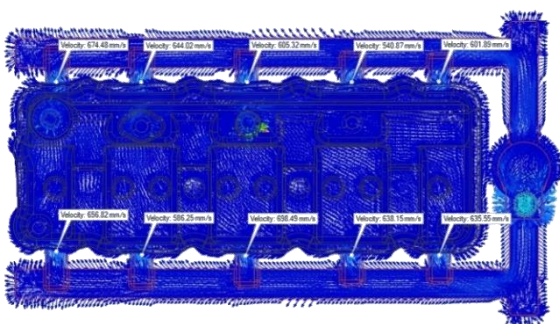


Fig. 14. Liquid metal velocities in gate section of sand casting

4.3. Cold shuts comparison die-casting

Cold shut can be explained as the case in which the liquid metal does not merge because of early solidification during the filling of the mold cavity through two separate channels. Thanks to the improvements made with the simulations, better results were obtained on

cold-shut surfaces by increasing the casting velocity. While the filling time is 1.08 s for the runner design of high-pressure die casting, the filling time of the runner design in sand casting is 5 s. By feeding the part from 10 gates, a more linear filling was provided, and a sleeve and riser were added to prevent early solidification. Therefore, the total weight in sand casting is heavier than that in high-pressure die casting. Figure 15 shows the positions and quantities of the cold shuts for HPDC.

Figure 16 shows the positions and quantities of cold shuts for SC. It was observed that the cold shuts were significantly less in HPDC than in the SC method.

Figure 17 shows a comparison of the number of maximum cold-shut points. Figure 18 shows a comparison of the solidification times.

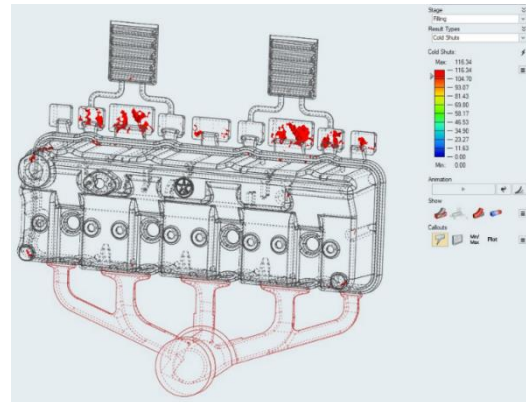


Fig. 15. Positions and quantities of cold shuts for HPDC

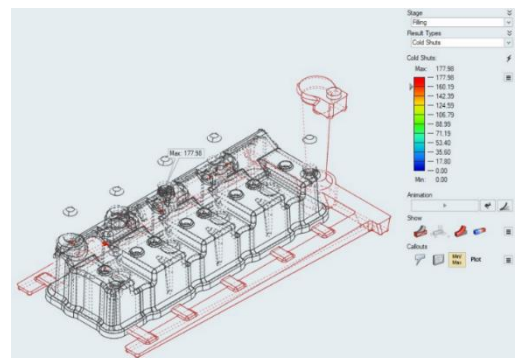


Fig. 16. positions and quantities of cold shuts for SC

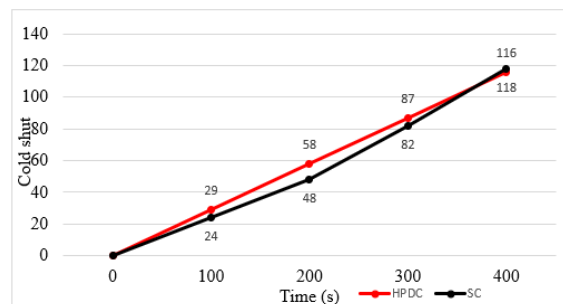


Fig. 17. Comparison of quantities for cold shut points in HPDC and SC

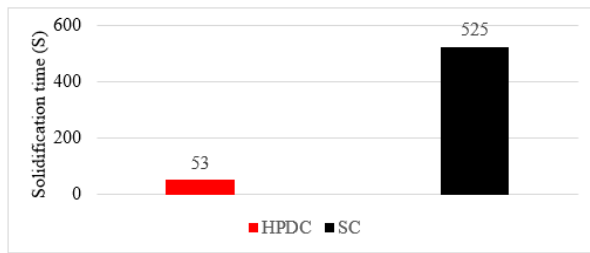


Fig 18. Comparison of the solidification time

4.4. Final air quantity comparison

In the high-pressure die casting process, filling takes very short periods; therefore, the air that fills the mold cavity is trapped in the liquid metal. The design uses chill vent pockets to remove trapped air from the liquid metal. In simulations where air pockets were not added, it was observed that there was too much oxide in the casting part. To ensure a non-air-trapped solution, thus trapped air inside the casting part causes porosity, air pockets were used in the runner design. The simulation parameter showing the final number of air shows where the air will or can be trapped. Since filling the liquid in the sand mold casting process occurs depending on the casting weight, the air that has filled the mold cavity is trapped in the liquid metal and rises to the upper parts of the casting part. A sleeve and riser were used to remove the air-trapped liquid metal from the casting part. A sleeve and riser were used in the design to remove trapped air from the liquid metal. Usage of the sleeve and riser not only will keep the part away from cold shutdown errors but also trap the final air inside the feeder. As in the high-pressure die casting, a high amount of oxide was observed in the casting part when the simulation was performed without the use of a sleeve and riser. Figure 19 shows the final air for HPDC, and Figure 20 shows the final air for SC. Considering the final air quantities, the oxides are transmitted to the ventilation pockets with the help of the liquid metal. HPDC gives slightly better results than the SC method.

4.5. Comparison of porosity

Microporosity can be defined as the voids created by gases during solidification, while macroporosity occurs due to material shrinkage during the same process. Specifically, Figure 21 displays areas with high macroporosity for High-Pressure Die Casting (HPDC), and Figure 22 illustrates high macroporosity regions for

Sand Casting (SC). On the other hand, Figure 23 depicts high microporosity areas for HPDC, and Figure 24 showcases high microporosity regions for sand casting.

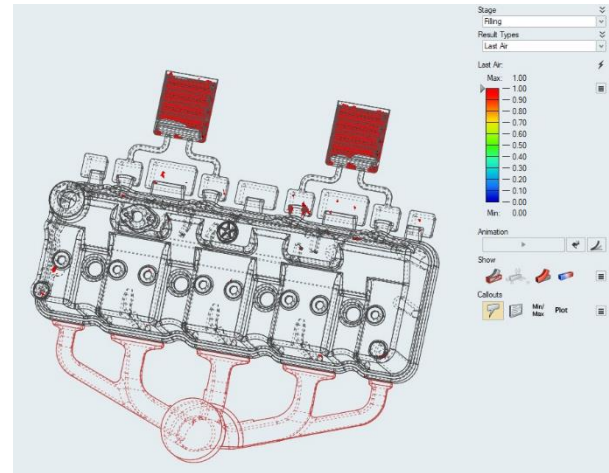


Fig. 19. High pressure die casting for final air

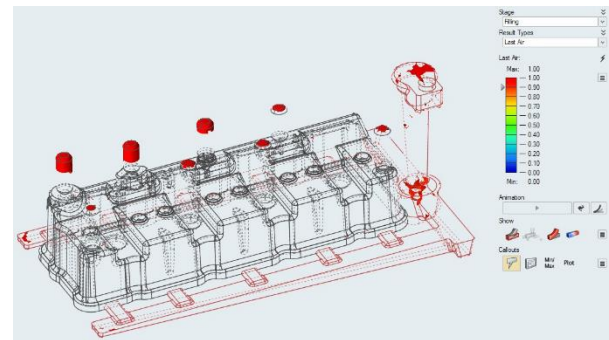


Fig. 20. Sand casting for final air

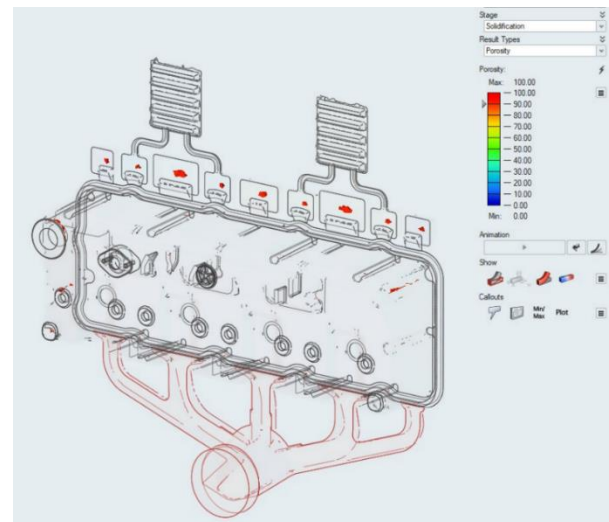


Fig. 21. High macroporosity areas for high pressure die casting

We must acknowledge that the higher mass is not solely attributed to this factor; according to production constraints in sand casting, part thickness should be greater than in high-pressure die casting. Additionally, the high-pressure die-cast method exhibits lower rejection rates in terms of macroporosity quantities.

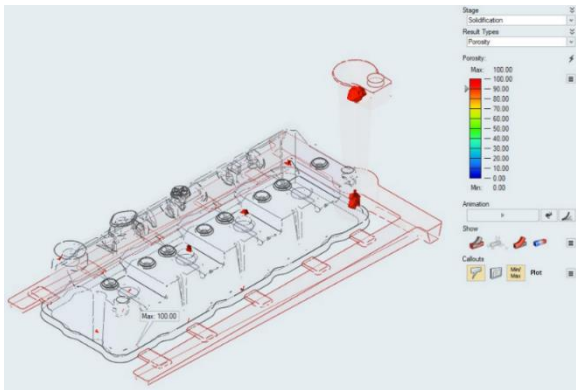


Fig. 22. High macroporosity areas for sand casting

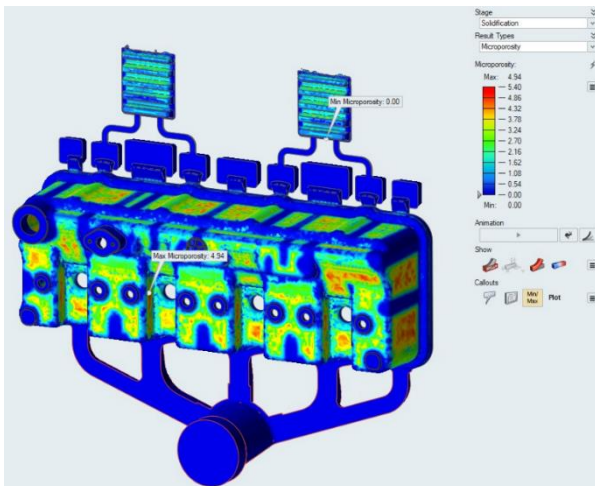


Fig. 23. High microporosity areas for high pressure die casting

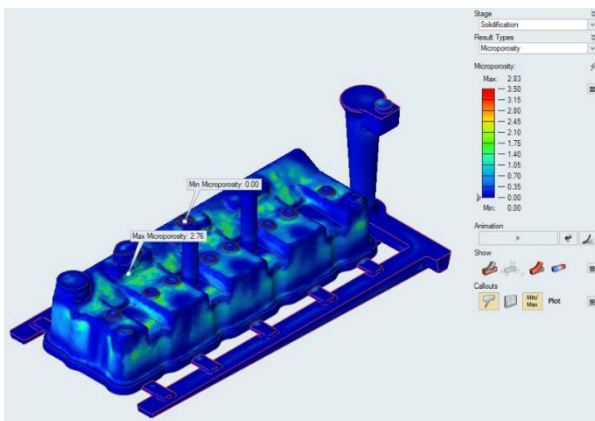


Fig. 24. High microporosity areas for sand casting

From the perspective of the microporosity index, as indicated in the literature and market research, values between 0 and 1 are considered perfect, between 1 and 2 are considered good, between 2 and 5 are considered medium, and values exceeding 5 are deemed bad. Figure 25 presents a comparison of the microporosity index for High-Pressure Die Casting (HPDC) and Sand Casting (SC).

The scrap weight ratio was determined by dividing the total weight of the runner and other casting process sections by the total weight of

the entire casting. In the sand-casting method, the scrap rate was 48.9%, while in high-pressure casting, it was calculated at 43.9%.

Notably, the costs associated with high-pressure casting are considerably higher than those in sand casting due to the utilization of a metal die. High-Pressure Die Casting becomes economically feasible when the total annual production exceeds 2150 pieces. Unfortunately, specific cost details are not provided due to confidentiality concerns.

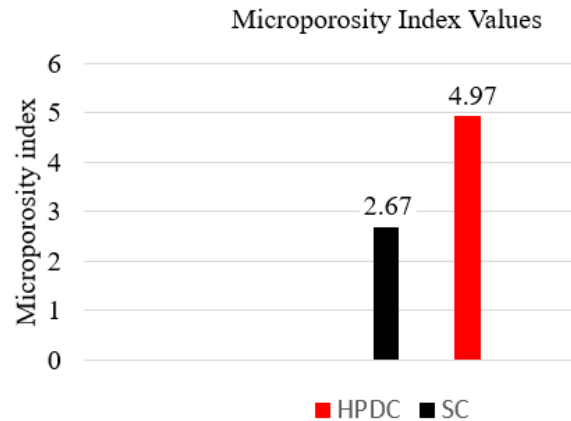


Fig 25. Comparison of microporosity index values

5. Conclusion

In this study, casting simulations were conducted using High-Pressure Die Casting (HPDC) and Sand Casting (SC) methods for the valve cover of a tractor engine. Through these simulations, the optimal casting method for producing the aluminum alloy valve cover was determined. To expedite the analysis process, some initial calculations were performed manually.

For both production methods, the optimum runner design was established with the assistance of simulations. Favorable outcomes were achieved by modifying the gate cross-section, the number of gates, and the width and depth of the runner in the high-pressure die casting simulation. This optimized runner design facilitated problem-free part production. In sand casting simulations, challenges such as cold junction points, final air content, and early solidification were identified and addressed by adjusting the number of feeders, risers, and gate section thickness to optimize the runner.

Considering the simulation results and cost calculations, High-Pressure Die Casting (HPDC) was deemed the most viable production method for the valve cover. HPDC

resulted in a total casting weight 39.7% lighter than that of Sand Casting, and the latter required a higher percentage of machining. Furthermore, it is anticipated that improved results can be achieved with the use of conditioner and vacuum applications in HPDC.

In sand casting, employing dry sand molding instead of green sand molding is expected to increase mold temperature, potentially leading to better outcomes for issues such as cold shut points and mold erosion.

6. References

1. Suresha S, Pawan H. Numerical simulation aided design of heat sink using Z-cast. *Mater Today Proc*, vol. 45, Elsevier Ltd; p. 404–11, 2020.
<https://doi.org/10.1016/j.matpr.2020.12.758>.
2. Papai J. Contact heat transfer coefficients in aluminum alloy die casting: An experimental and numerical investigation. Doctoral dissertation. Ohio State University, 1994.
3. Patnaik L, Saravanan I, Kumar S. Die casting parameters and simulations for crankcase of automobile using MagmaSoft. *Mater Today Proc*, vol. 22, Elsevier Ltd; p. 563–71, 2020.
<https://doi.org/10.1016/j.matpr.2019.08.208>.
5. Jadhav AR, Hujare DP, Hujare PP. Design and optimization of gating system, modification of cooling system position and flow simulation for cold chamber high pressure die casting machine. *Mater Today Proc*, vol. 46, Elsevier Ltd; p. 7175–81, 2021.
<https://doi.org/10.1016/j.matpr.2020.11.346>.
5. Ramnath BV, Elanchezian C, Chandrasekhar V, Kumar AA, Asif SM, Mohamed GR, et al. Analysis and Optimization of Gating System for Commutator End Bracket. *Procedia Materials Science*, 6:1312–28, 2014.
<https://doi.org/10.1016/j.mspro.2014.07.110>.
6. Sulalman S, Chee Keen T, Pertanian Malaysia U, Malaysia S. Flow analysis along the runner and gating system of a casting process. vol. 63. 1997.
7. Kumar R, Madhu S, Aravindh K, Jayakumar V, Bharathiraja G, Muniappan A. Casting design and simulation of gating system in rotary adaptor using Procast software for defect minimization. *Mater Today Proc*, vol. 22, Elsevier Ltd; p. 799–805, 2020.
<https://doi.org/10.1016/j.matpr.2019.10.156>.
8. Dai X, Yang X, Campbell J, Wood J. Effects of runner system design on the mechanical strength of Al-7Si-Mg alloy castings. *Materials Science and Engineering A*, 354:315–25, 2003.
[https://doi.org/10.1016/S0921-5093\(03\)00021-2](https://doi.org/10.1016/S0921-5093(03)00021-2).
9. Hu BH, Tong KK, Niu XP, Pinwill I. “Design and optimisation of runner and gating systems for the die casting of thin-walled magnesium telecommunication parts through numerical simulation”, *Journal of Materials Processing Technology*, 105(1-2):128-133, 2000.
10. Zheng K, Lin Y, Chen W, Liu L. Numerical simulation and optimization of casting process of copper alloy water-meter shell. *Advances in Mechanical Engineering*, 12, 2020.
<https://doi.org/10.1177/1687814020923450>.
11. Dubey S, Swain SR. Numerical investigation on solidification in casting using ProCast. *IOP Conf Ser Mater Sci Eng*, vol. 561, Institute of Physics Publishing; 2019.
<https://doi.org/10.1088/1757-899X/561/1/012049>.
12. Long A., Thornhill D., Armstrong C. and Watson D., The Impact of Die Start-Up Procedure for High Pressure Die Casting. *SAE International Journal of Materials and Manufacturing*. Vol. 6, No.3, June 2013.
<https://doi.org/10.4271/2013-01-0829>
13. Andresen, B., “Die Casting Engineering”. New York: Marcel Dekker, ISBN : 0-8247-5935-4, 2005.
14. Klobcar, D and Tusek, J. “Thermal stresses in aluminum alloy die casting dies”. *Computation Materials Science*. 43, 2008.
<https://doi.org/10.1016/j.commatsci.2008.03.009>